Science of the Total Environment 836 (2022) 155477

Contents lists available at ScienceDirect

Science of the Total Environment

journal homepage: www.elsevier.com/locate/scitotenv

What are the likely changes in mercury concentration in the Arctic atmosphere and ocean under future emissions scenarios?

Amina T. Schartup [a,*], Anne L. Soerensen [b], Hélène Angot [c], Katlin Bowman [d], Noelle E. Selin [e]

[a] Scripps Institution of Oceanography, University of California at San Diego, La Jolla, CA 92093, USA
[b] Department of Environmental Research and Monitoring, Swedish Museum of Natural History, Stockholm, Sweden
[c] Extreme Environments Research Laboratory, École Polytechnique Fédérale de Lausanne (EPFL) Valais Wallis, Sion, Switzerland
[d] University of California Santa Cruz, Ocean Sciences Department, 1156 High Street, Santa Cruz, CA 95064, USA
[e] Institute for Data, Systems, and Society, and Department of Earth, Atmospheric, and Planetary Sciences, Massachusetts Institute of Technology, 77 Massachusetts Avenue [E17-381], Cambridge. MA 02139, USA

HIGHLIGHTS

- Arctic mercury concentrations respond to changes in emissions and environmental change.
- Modeling shows rapid mercury deposition decline with aggressive reduction measures.
- Delaying action will limit the impact of mercury emission reduction measures.
- Until 2050, mercury emissions influence ocean mercury concentrations more than environmental change scenarios.
- There is a need for prompt and ambitious action to reduce mercury concentrations in the Arctic.

GRAPHICAL ABSTRACT

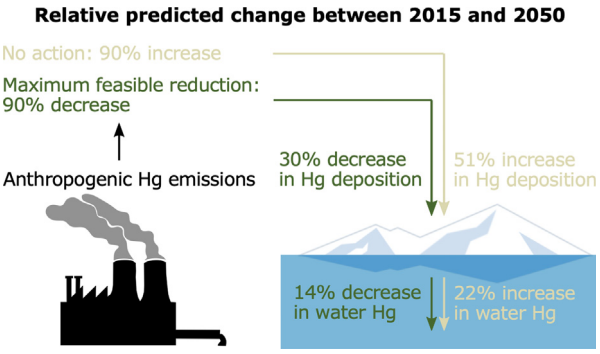

ARTICLE INFO

Editor: Zhouqing Xie

Keywords:
AMAP
Hg
Deposition
Climate change
Policy
Box model

ABSTRACT

Arctic mercury (Hg) concentrations respond to changes in anthropogenic Hg emissions and environmental change. This manuscript, prepared for the 2021 Arctic Monitoring and Assessment Programme Mercury Assessment, explores the response of Arctic Ocean Hg concentrations to changing primary Hg emissions and to changing sea-ice cover, river inputs, and net primary production. To do this, we conduct a model analysis using a 2015 Hg inventory and future anthropogenic Hg emission scenarios. We model future atmospheric Hg deposition to the surface ocean as a flux to the surface water or sea ice using three scenarios: No Action, New Policy (NP), and Maximum Feasible Reduction (MFR). We then force a five-compartment box model of Hg cycling in the Arctic Ocean with these scenarios and literature-derived climate variables to simulate environmental change. No Action results in a 51% higher Hg deposition rate by 2050 while increasing Hg concentrations in the surface water by 22% and <9% at depth. Both "action" scenarios (NP and MFR), implemented in 2020 or 2035, result in lower Hg deposition ranging from 7% (NP delayed to 2035) to 30% (MFR implemented in 2020) by 2050. Under this last scenario, ocean Hg concentrations decline by 14% in the surface and 4% at depth. We find that the sea-ice cover decline exerts the strongest Hg reducing forcing on the Arctic Ocean while increasing river discharge increases Hg concentrations. When modified together the climate scenarios result in a ≤5% Hg decline by 2050 in the Arctic Ocean. Thus, we show that the magnitude of emissions-induced future changes in the Arctic Ocean is likely to be substantial compared to climate-induced effects. Furthermore, this study underscores the need for prompt and ambitious action for changing Hg concentrations in the Arctic, since delaying less ambitious reduction measures–like NP–until 2035 may become offset by Hg accumulated from pre-2035 emissions.

* Corresponding author.
E-mail address: achartup@ucsd.edu (A.T. Schartup).

http://dx.doi.org/10.1016/j.scitotenv.2022.155477
Received 31 December 2021; Received in revised form 12 April 2022; Accepted 19 April 2022
Available online 23 April 2022

1. Introduction

In this paper, we explore the potential changes in mercury (Hg) concentrations in the Arctic atmosphere and ocean under future Hg emissions and simplified climate scenarios. The work was prepared for the 2021 Arctic Monitoring and Assessment Programme Mercury Assessment (AMAP, 2021).

Future changes in Hg concentration in the Arctic atmosphere and ocean will result from multiple, interacting societal and environmental phenomena. The amount of Hg which will be present in the Arctic in the future depends not only on how Hg emissions and releases change with time but also on emissions of other pollutants, which affect atmospheric chemical interactions, and on the change in global and regional climate. Emissions of pollutants (including Hg) as well as greenhouse gases are shaped by global and regional trajectories involving economic activities, energy use, regulatory constraints, and the availability and application of technologies. Assessing likely changes in Hg concentrations thus requires examining potential changes in these underlying drivers, the resulting emissions, and the environmental and climate interactions that affect Hg transport and fate in the Arctic ecosystem.

Changes in Hg concentration in the Arctic atmosphere and ocean will take place on different time scales. Short-term timescales (i.e., over the next few years) are relevant for near-term decision-making, including the first effectiveness evaluation of the Minamata Convention, which will be carried out by 2023; atmospheric models can simulate the influence of changing emissions in the present and near future. In the medium term (i.e., over the next several years to a few decades), enhancements in legacy emissions from current as well as future emissions will play a substantial role (Amos et al., 2013). The degree of climate change occurring in the medium term (i.e., over the next few decades until 2050) has largely been determined by existing greenhouse gas trajectories. In the longer term (i.e., beyond 2050), trajectories of future greenhouse gas emissions will play a substantial role in determining Arctic climate, and combined with continued anthropogenic Hg emissions, will further influence Hg concentrations.

The relative importance of primary emissions, legacy emissions, and climate changes to Hg concentrations differs depending on these timescales; previous efforts have not consistently accounted for these different processes. For the atmosphere, in the short term (i.e., over an individual year), concentration changes and Hg deposition will follow changes in emissions in different regions and their relative contributions and can be calculated based on source-receptor information. Many previous modeling efforts to quantify the impacts of changes in deposition to global regions (e.g., Corbitt et al., 2011; Chen et al., 2014; Travnikov et al., 2017) have simulated these dynamics. For the ocean, the timescales of ocean circulation may result in a lag relative to changes in the atmosphere, but many of these changes will overlap. In the medium term (i.e., years to decades), enhancements in current and future emissions can be accounted for using dynamical biogeochemical cycle models and coupled ocean-atmosphere models (Angot et al., 2018; Selin, 2018). For timescales of decades and longer, ecosystem changes due to climate change will influence the global Hg cycle (Obrist et al., 2018), and these influences will also affect the Arctic; assessing them requires quantifying future climate change trajectories and applying process-based models that account for ecosystem changes.

Mercury concentrations in the Arctic Ocean are the result of past and current emissions and processes such as atmospheric deposition, riverine inputs, biotic and abiotic transformations, and settling to the deep ocean enabled by the biological pump. When evaluating future trends in ocean Hg concentrations, it is important to not only consider trends in industrial activities and national and global policies that influence Hg emissions, and by extension depositions on the surface ocean, but also consider how concomitant climatic and environmental shifts may exacerbate or dampen seawater Hg concentrations. Biogeochemical models can be used to consider these simultaneous changes and provide integrated estimates of future trends. The ultimate forward-looking model of Hg cycling will be able to combine emission scenarios, climate change simulations and speciated Hg modeling to produce future trends. But because of a limited understanding of how Hg inputs from sources other than the atmosphere will change (e.g., rivers, erosion) this model does not yet exist. However, currently available models can: (1) generate projections based on future anthropogenic deposition scenarios, assuming that other fluxes and processes are constant; and (2) consider the effects of some large-scale climate-related changes (e.g., increased freshwater discharge, permafrost thaw, melting of ice caps or reduction of sea ice extent) on Hg fluxes. These models can also be used to compare the relative impact of policy decisions.

Here, we explore potential changes in Hg concentrations in the Arctic atmosphere and ocean under future Hg emissions scenarios, by examining possible trajectories over the next few decades (i.e., until 2050). In doing so, we also survey the state of the science on differentiating the impact of direct emissions and accounting for their further biogeochemical cycling in the context of other drivers, such as climate change. A key contribution of this study is to better quantify the importance for Arctic Hg concentrations of primary Hg emissions relative to other changes, including climate and legacy emissions changes. This study applies a systems approach, evaluating trajectories of Hg concentrations in the context of assumptions about anthropogenic Hg emissions pathways, many of which contribute to uncertainty and variability in future projections and some of which can be determined by future decisions. In the following sections, existing anthropogenic Hg emissions scenarios are compared, with particular attention to the assumptions they make about underlying socio-economic trajectories and emissions control policies, including for greenhouse gases. Next, a range of changes in future Hg concentrations in the Arctic atmosphere are projected using one set of future Hg emissions scenarios, accounting for the direct anthropogenic emissions and legacy impacts that may affect the Arctic in the short and medium term until 2050; quantitative results are compared with previous literature that evaluated the impact of climatic changes on Hg emissions and concentrations in the longer term. Atmospheric deposition from these short- and medium-term scenarios is then used to drive an ocean model. We conclude by discussing the potential for different emissions trajectories to affect Arctic concentrations in the short, medium, and long term; we also make recommendations regarding the model development and research needed to improve the simulation of future Hg scenarios.

2. What are the future anthropogenic emissions scenarios when comparing existing literature estimates?

Several efforts have been made to project global and regional anthropogenic Hg emissions into the future (Table S1); these differ not only on the potential trajectories of future Hg but also on their underlying assumptions, base years, and temporal and spatial extent. The processes that affect the emission of Hg globally also contribute to the emission of other pollutants (e.g. sulfur dioxide (SO_2), nitrogen oxides (NO_x), black carbon), including greenhouse gases. Anthropogenic emission scenarios for Hg thus require assumptions of underlying socio-economic activities, and some build upon scenarios that have been developed and used to understand greenhouse gas emissions and global climate change.

Scenarios have been developed to facilitate analysis of the pollution implications of different global socio-economic trajectories (Hayhoe et al., 2017). Most of the anthropogenic emission scenarios that exist for Hg rely on the underlying socio-economic assumptions from the Intergovernmental Panel on Climate Change (IPCC)'s Special Report on Emissions Scenarios (SRES; IPCC, 2000). The SRES scenarios are emissions-based and capture "storylines" (A1, A2, B1, B2) which provide illustrative trajectories of socio-economic and technological change (four sets of scenarios called "families"). The scenarios in the group denoted A1 (A1B; balanced and A1FI; fossil-fuel intensive) represent a future characterized by rapid economic growth and a convergence across regions but differ in their specifications of technological change (i.e., the A1FI scenario is more fossil-fuel intensive than A1B); not explicitly discussed here are the scenarios A1T (which assumes the use of predominantly non-fossil energy sources) and A2 (which assumes more fragmented economic growth and technological

development than other storylines). In the scenarios in the group denoted B, the B1 scenario includes reductions in material intensity under a globalized service-oriented economy, while the B2 scenario emphasizes local sustainability solutions. Importantly, none of the SRES scenarios includes any sort of policies or measures to limit climate change. More recent analysis of socio-economic trajectories and climate change policies have built upon the Representative Concentration Pathways (RCP) outlined in the IPCC Fifth Assessment Report (AR5; IPCC, 2014); these are radiative forcing scenarios and reflect climate policies that incorporate lower warming targets. Associated Shared Socio-economic Pathways (SSP) were developed and constrained to create scenarios that can be used in impact, adaptation, and vulnerability analysis (Riahi et al., 2017). However, widely applied Hg emissions scenarios have not been built upon these more recent global-scale scenarios. This means that most future projections of anthropogenic Hg emissions are not strictly comparable to those which address other pollutants, or with associated projections of climate change. This challenges the interpretation of and comparison between the magnitudes of the concentrations change of other pollutants projected as a result of future climate scenarios, which have been assessed in a few studies, and those in studies which project Hg concentrations. This is discussed further below.

With respect to Hg in particular, comparisons between future emissions scenarios are made more difficult because existing scenarios build from different base year inventories, make different assumptions regarding underlying activities, and specify different rates of application and varying efficiencies of air pollution and Hg-specific control technologies. These assumptions affect the total amount of Hg emitted as well as its speciation. When it comes to global emissions scenarios, there are large differences in projections, which are driven not only by differences in the scenarios but also by base case assumptions. Existing future Hg emissions scenarios from previous literature are summarized in Table S1; the projections of global anthropogenic Hg emissions from the different scenarios are shown in Fig. 1.

Streets et al. (2009) used a base year of 2006 (2480 Mg) and projected Hg emissions to 2050 under four different SRES scenarios (A1B, A2, B1 and B2). Beginning with 2006, global emissions increase under the A1B, A2 and B2 scenarios (by 96%, 57% and 6%, respectively) and decrease slightly under the B1 scenario (by 4%). They found that in developing countries, coal combustion is the largest cause of emission increases; they also calculated that the application of an activated carbon injection (ACI) system on all coal-fired power plants could lower the range of emissions over the different scenarios from 2386–4856 Mg to 1670–3840 Mg. Lei et al. (2014) also projected Hg emissions using IPCC SRES scenarios (A1B, B1 and A1F1); global emissions in 2050 range from 2390 to 5990 Mg, a 9% to 173% increase over a base year of 2000 (2190 Mg; from Pacyna et al., 2006). Rafaj et al. (2013) projected emissions for Hg beginning from a 2010 base year using the International Institute for Applied Systems Analysis (IIASA) Greenhouse Gas and Air Pollution Interactions and Synergies (GAINS) model under scenarios of energy consumption with no greenhouse gas mitigation efforts and with climate policies which aim to limit the global temperature rise to within 2 °C of pre-industrial levels. For these underlying activity scenarios, they examined two different sets of air pollution and Hg control measures: (1) current legislation to control air pollution by 2030 and no further effort between 2030 and 2050; and (2) a Maximum Feasible Reduction (MFR) scenario assuming the full adoption of the best available technologies. Under the base case scenario (BAS), emissions increase from 1554 Mg in 2010 to 2661 Mg in 2050; Hg emissions are reduced to ~850 Mg under the scenario consistent with a below 2 °C temperature goal (CLIM) and to ~620 Mg if air pollution legislation and climate policies are adopted in parallel (CLIM-MFR scenario). Pacyna et al. (2016) projected future activities and emissions reduction scenarios to 2035, under current policies (CP), new policies (NP) and MFR scenarios. They adopted underlying activity rates from the World Energy Outlook and based their estimates on economic projections and other trends. Under the CP scenario, emissions increase from 1885 Mg in 2010 to 1960 Mg in 2035; Hg emissions are reduced to 1020 Mg and 300 Mg under the NP and MFR scenario, respectively.

Regional studies have provided additional scenarios for key source regions of importance to deposition in the Arctic and have shown that socio-economic assumptions embedded within emissions scenarios, as well as climate and energy policies, have a large impact on the overall trajectory of Hg emissions, compared with the impact of differences in application of control technologies. Giang et al. (2015) designed scenarios for the power sector in India and China based on activity use in the A1B and B1 scenarios and with a no additional control (NAC) and two different end-of-pipe (EOP) control technology scenarios consistent with Minamata Convention requirements. They found that the underlying assumptions about energy use (especially coal use) had a larger effect on emissions from the sector in question than the application of control technology.

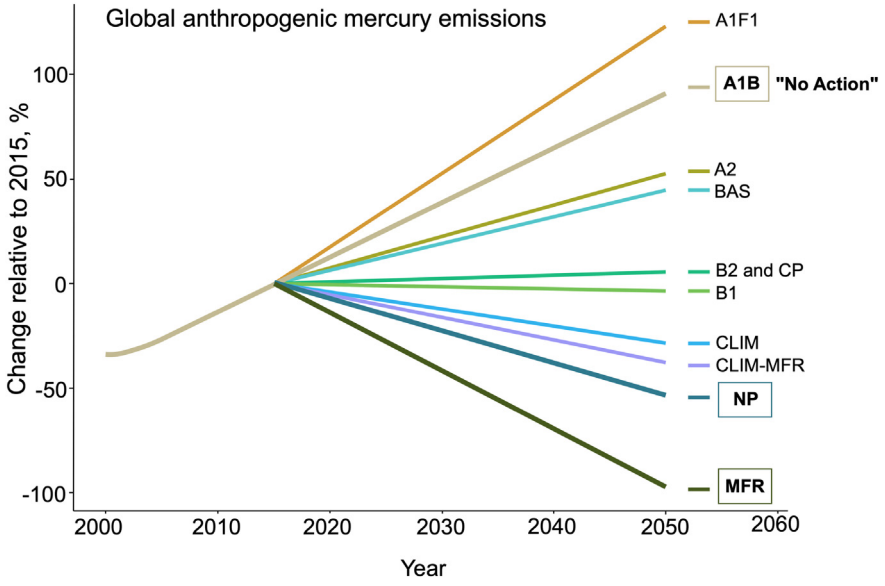

Fig. 1. Global anthropogenic emissions projections under different scenarios. Scenarios that started before 2015 are linearly interpolated and extrapolated to 2050 (assuming constant annual growth or decrease). Emissions for 2000–2008 are from Streets et al. (2009) while emissions for 2009–2015 correspond to an A1B scenario. Current Policy (CP), New Policy (NP) and Maximum Feasible Reduction (MFR) scenarios are from Pacyna et al. (2016). A1B, A2, B1 and B2 scenarios are from Streets et al. (2009). BAS, CLIM and CLIM-MFR are from Rafaj et al. (2013). A1F1 scenario is from Lei et al. (2014). The framed scenarios are used in the modeling below.

Rafaj et al. (2014) compared a baseline scenario for Europe with a scenario including the highest possible electricity generation from renewables by 2050. They found that co-control technologies used to abate air pollutants reduce Hg emissions by 35% to 45% and that the largest fraction of emissions cuts under the MFR scenario are attributed to the deployment of renewables in the power sector. Mulvaney et al. (2020) examined interactions between the Paris Agreement and Minamata Convention requirements under seven different scenarios that combined climate policies and end-of-pipe control policies to the year 2030. They found that climate policies consistent with the Paris Agreement in China can serve to mitigate Hg levels when implemented together with the Minamata Convention, with an additional 5% reduction under more ambitious climate goals simulated.

3. What are the predicted changes in mercury concentrations in the atmosphere?

For this study, we conduct a model analysis using the present-day (2015; BASE simulation) AMAP/UNEP 2015 inventory developed for the latest Global Mercury Assessment (AMAP/UNEP, 2019) and future anthropogenic Hg emission scenarios from Pacyna et al. (2016) to simulate a range of potential changes in Arctic atmospheric Hg concentrations (Fig. 1; framed scenarios are used here, and Table S1). These scenarios are used to force the ocean model in Section 4 of this manuscript. The NP scenario assumes that policy commitments and plans to reduce greenhouse gas emissions are fully implemented. In this scenario, the use of Hg in products is reduced by 70%. This scenario assumes global emissions of ~1020 Mg/y. The MFR scenario assumes that all countries reach the highest feasible/available reduction efficiency in each emission sector (global emissions of ~300 Mg/y). It should be noted that the NP and MFR scenarios both assume a significant decrease of Chinese emissions, the main contributor to Hg deposition in the Arctic (AMAP, 2021; AMAP/UN Environment, 2019).

According to the source apportionment analysis performed by Dastoor et al. (this issue) and AMAP (2021) (Chapter 3), global natural and secondary emissions are the main contributors to Hg deposition in the Arctic (~70%). Using a global box model framework, Chen et al. (2018) showed that present-day Hg deposition over the Arctic Ocean is mainly from historical anthropogenic emissions from Asia (31%), followed by North America (18%), South America (12%), the former USSR (12%) and Europe (11%). Hg deposition due to primary anthropogenic emissions is mostly due to emissions in East Asia (~33%; China, Korea and Japan). Europe, Southeast Asia, South Asia, Sub-Saharan/sub-Sahel Africa, South America, and Russia/Belarus/Ukraine each contribute ~7% to ~9%. Anthropogenic emissions north of 66°N currently only contribute ~2% of Hg deposition in the Arctic. As a result of these source contributions, trajectories for Asia will likely be the most influential for future Arctic deposition, especially since future global emissions trajectories are greatly affected by Asia's emissions. While local source increases may be important for other pollutants such as aerosols and ozone (see, for example, Marelle et al., 2018), they are unlikely to become future sources in the Arctic.

According to the model ensemble (AMAP, 2021: Chapter 3, Dastoor et al. (this issue)), the annual mean atmospheric Hg(0) concentration in the Arctic (north of 60°N) is 1.4 ng/m^3 (BASE scenario). Note that the BASE scenario refers to simulations performed using the year 2015 AMAP global anthropogenic emissions inventory developed for the 2018 Global Mercury Assessment. This mean Hg(0) concentration drops to 1.2 and 1.1 ng/m^3 assuming global anthropogenic emissions of ~1020 Mg/y (NP scenario) or ~300 Mg/y (MFR scenario), respectively. The impact of different regulatory strategies is of the same order of magnitude for both Hg(0) concentrations and atmospheric deposition. Hereafter, we focus on deposition since it is the main pathway of Hg transfer from the atmosphere to the ocean and ecosystems. The best-case estimate shows the potential for short-term reductions: that is, it illustrates the maximum possible impact of the primary emissions reduction scenario without accounting for changes in legacy emissions. Under the NP case, deposition to Arctic land decreases from 6.9 μg/m^2/y under the BASE case to 5.6 μg/m^2/y (i.e., a 19% reduction of Hg deposition), and to the Arctic Ocean from 7.4 μg/m^2/y to 6.1 μg/m^2/y (i.e., a 18% reduction of Hg deposition; Fig. 2). The MFR scenario reduces Arctic deposition further, to 5.0 μg/m^2/y and 5.4 μg/m^2/y to land and ocean, respectively (i.e., a 28 and 27% reduction of Hg deposition, respectively).

To investigate how delays in implementing anthropogenic Hg emission reductions and the associated growing legacy Hg reservoir affect deposition fluxes to the Arctic, we followed the methodology of Angot et al. (2018). Because the parameterization of this effect is challenging, many global-scale chemical transport models (CTMs) hold legacy emissions constant while changing future anthropogenic Hg emission scenarios. Fully accounting for legacy emissions requires coupled atmosphere-ocean-land models that are not widely accessible and are extremely computationally intensive. To account for the effect of legacy emissions, Angot et al. (2018) developed a methodology that links CTM simulations with biogeochemical cycle modeling, which adjusts legacy deposition flux to account for future increases. To accomplish this, the impact of legacy emissions is isolated using a sensitivity simulation in the model; the resulting spatially resolved deposition flux is scaled based on the global average increase of legacy emissions calculated using the fully coupled biogeochemical cycle model. This method allows calculation of the magnitude of changes in the legacy component of deposition in a spatially resolved way but assumes that its distribution does not change from the present day. To estimate the impacts of delay, we assume that anthropogenic Hg emissions grow following the trajectory of a No Action scenario (+55.9 Mg/y; constructed based on the A1B scenario by Streets et al., 2009) until implementation of a NP or MFR scenario. This A1B scenario assumes rapid increases in energy use and economic growth, low population growth, continued globalization, and rapid introduction of new and more efficient technologies.

Fig. 2 shows deposition when NP an MFR are implemented in 2015, 2020, and 2035. It shows that the relative impact of NP or MFR policy on Arctic deposition decreases by ~50% or ~35%, respectively, for each 5-year delay. Under a 20-year delay in both the NP and MFR cases, the effect

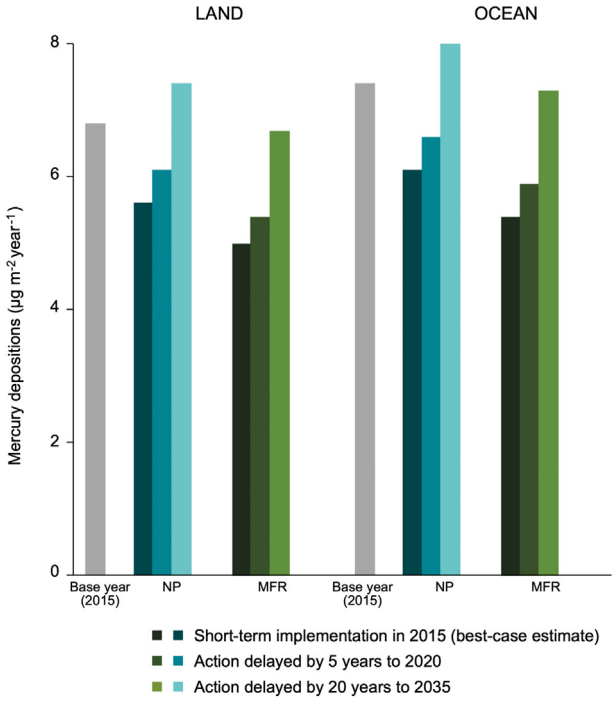

Fig. 2. Mercury deposition flux to land and ocean areas of the Arctic (north of 60°N; in μg/m^2/y) using future emissions scenarios and assuming a short-term or delayed implementation by 5 and 20 years of global mitigation efforts. Base year (2015) Hg (gray bar) deposition fluxes are from the model ensemble (AMAP, 2021: Chapter 3). The blue bars represent Hg deposition under the New Policy (NP) scenario and green bars are deposition under the Maximum Feasible Reduction (MFR) scenario.

of added emissions to the legacy pool during that 20-year period entirely offsets the reductions to primary emissions that occur later.

Fig. 3A and B illustrate the relative change in Hg deposition over the Arctic Ocean under the three policy scenarios. Fig. 3A shows the time trend between 1850 and 2050 used in this study to drive the ocean model. Since there is no Arctic Ocean specific time series, we produced one by forcing the global box model published by Amos et al. (2013) with the different emission scenarios and delays in implementation. Amos et al. (2013) model produces global depositions which we convert into change terms relative to 2015 and assume that similar changes in depositions occur over the Arctic Ocean. However, when comparing Figs. 3A and 2 we see that the global depositions underestimate the impacts of delayed action. Angot et al. (2018) suggested that this difference is due to remote regions being more influenced by global rather than local emissions and thus carry a stronger legacy emissions penalty. Fig. 3B isolates the relative change in Hg deposition between 2015 and 2050 from the time series in Fig. 3A. We see that the No Action scenario (A1B) results in a 51% higher Hg deposition rate by 2050. Both "action" scenarios (NP and MFR) result in reductions in Hg deposition ranging from 7% (for NP delayed by 20 years to 2035) to 30% (for MFR, delayed by 5 years, thus implemented in 2020).

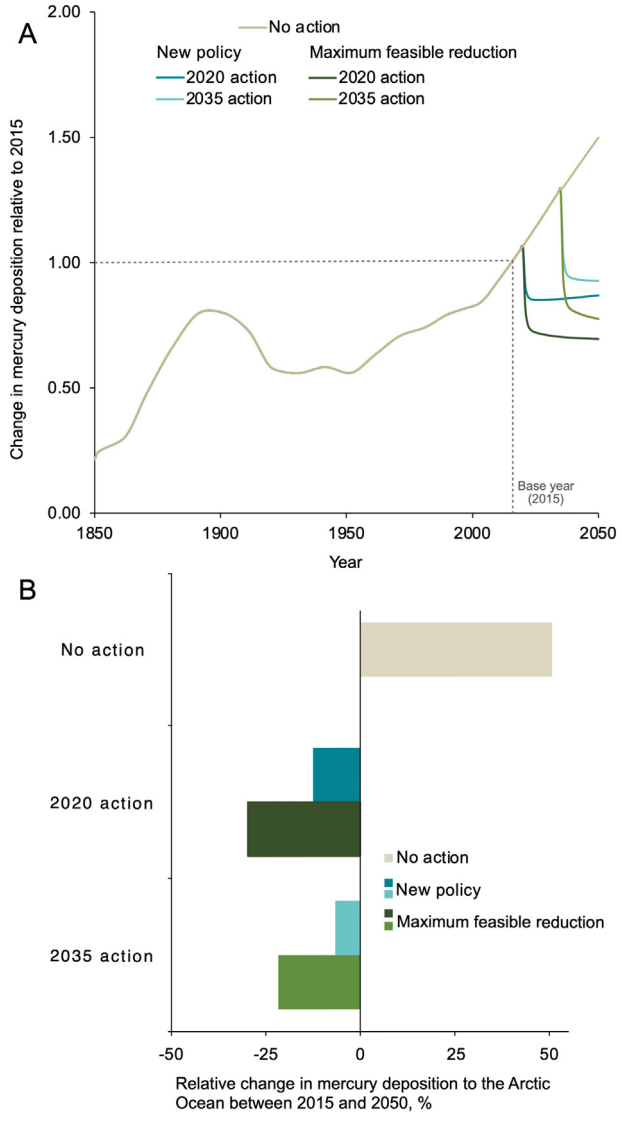

Fig. 3. Changes in mercury deposition on the Arctic Ocean. A. Hg deposition from 1850 to 2050 relative to Base Year (2015) used to drive the Arctic Ocean mercury box model. No Action (A1B) scenario (cream; Streets et al., 2009), the New Policy (blue; Pacyna et al., 2016), and Maximum Feasible Reduction (green; Pacyna et al., 2016) scenarios implemented in years 2020 and 2035. B. Bars represent the relative change in Hg deposition on the Arctic Ocean surface in three scenarios.

The atmospheric changes prompted by changes in anthropogenic Hg emissions can be compared with the magnitude of changes expected from climate change, in the short, medium and long term. Lei et al. (2014) estimated the relative contribution of anticipated anthropogenic Hg emission and climate change on U.S. atmospheric Hg levels. They found that anthropogenic emissions would deliver 32–53% while climate and natural emission would contribute 47–68% of projected changes by 2050. The Arctic Hg cycle is intrinsically linked to sea-ice extent, surface-atmosphere gas exchange, river exports, permafrost extent, and seasonal snow depth (Macdonald, 2005; Obrist et al., 2018; Schuster et al., 2018; St Pierre, 2018; Stern, 2012), all of which are expected to change in the future. For example, using a modeling approach, Dastoor et al. (2015) showed that an increase in net deposition in the Arctic under climate change is primarily driven by changes in snowpack and sea-ice conditions. Changes in sea-ice dynamics may indeed shift how much Hg(0) is available for oxidation (Moore et al., 2014). Changes in sea ice extent could also affect atmospheric Hg depletion events (AMDEs), by changing the availability of reactive halogens (Douglas and Blum, 2019). It has also been suggested that air temperature changes can impact the timing of and thus deposition fluxes (Cole and Steffen, 2010). Climate change could also increase Hg emissions from wildfires by 14% globally and by 13% in Eurasia by 2050 (Kumar et al., 2018) resulting in increased Arctic Hg deposition (as wildfires contribute ~10% of the total annual Hg deposition to the Arctic; Kumar and Wu, 2019). In addition, tundra and permafrost soils serve as reservoirs of a large legacy pool of past and present Hg emissions that accumulated in the Arctic (Olson et al., 2018; Schuster et al., 2018; Lim et al., 2020) and climate-driven permafrost thaw could release significant amount of previously locked-away Hg (Schaefer et al., 2020). The greening of the Arctic will also likely impact air/surface exchanges (Grannas et al., 2013) and reduce the extent of re-emission of Hg from the cryosphere (Dastoor and Durnford, 2014; Dastoor et al., 2015). On the other hand, higher surface temperature may enhance the photo-reduction and re-emission of Hg from the Arctic Ocean, affecting atmospheric concentrations. Since accounting for these long-term ecosystem changes on Hg deposition would require yet-to-be-developed process-based models, here we limit our analysis of projected changes in Hg deposition to near-future (2050) changes in anthropogenic emissions.

4. What are the predicted changes in total mercury concentrations in the Arctic Ocean?

Since 2012, nine modeling studies on Hg in the Arctic Ocean (or global studies that include the Arctic Ocean) have been published. The models vary in resolution, spatial coverage and Hg species that are included. They also vary in design, falling into 3 categories: (1) box models; (2) slab-ocean models integrated into an atmospheric framework; and (3) global biogeochemical models of the ocean. The studies conducted using these models provide an initial quantitative assessment of important drivers of Hg concentrations and speciation in the Arctic Ocean. Table S2 gives an overview of these models and their major findings. Of the nine studies, only one reported projections for Hg concentrations in the Arctic Ocean (Chen et al., 2018). They did so using a global source-receptor model including a five-compartment Arctic box model based on Soerensen et al. (2016a).

Soerensen et al. (2016a) developed a mass budget for total Hg and the first budget for monomethylmercury (MMHg) and dimethylmercury (DMHg) in the Arctic Ocean; and showed that the upper part of the Arctic Ocean is very responsive to changes in Hg inputs. They used a box model to reassess the lifetime of Hg in the Arctic Ocean and reported that Hg takes 13 years to cycle out of the upper ocean (<200 m), and 45 years to cycle out of the deep Arctic Ocean (>200 m). The Arctic food web is highly dependent on planktonic activity in the upper ocean, suggesting that policy actions that reduce atmospheric deposition and Hg concentrations in the upper ocean can have a relatively rapid impact on the food web Hg burden.

The deeper central Arctic Ocean has a considerable lag in response to changing inputs to the surface ocean, which will also mean a slow response to future changes. Thus, both changes in the external forcing and changes to the lifetime of Hg in the different parts of the water column will control the Hg concentration in the future Arctic Ocean.

The main inputs of Hg to the Arctic Ocean from outside the Arctic are to the surface layer, such as atmospheric deposition or riverine discharge (Soerensen et al., 2016a; AMAP, 2021: Chapter 3 and Dastoor et al. (2022a, 2022b) for more information on sources of Hg to the Arctic). Atmospheric deposition is predicted to contribute 40% to 50% of external inputs (including deposition to snow and ice released during spring/summer) and rivers and coastal erosion contribute 50% to 55%. Soerensen et al. (2016a) showed how increasing atmospheric deposition between 1850 and 2010 had an almost equal response in the increase of surface water concentrations but propagated down the water column with a long lag time to the deep Arctic water. Chen et al. (2018) ran a range of future emissions scenarios (2015–2050) with all other parameters kept constant. Under a constant emission scenario, they found that a 12% increase in atmospheric Hg resulted in a 9% increase in Arctic Ocean Hg mass, while a "zero emissions" scenario resulted in a rapid 50% decline in Hg deposition but only a 10% Arctic Ocean Hg decline by 2050.

The importance of rivers as a source of Hg to the Arctic Ocean was demonstrated by Fisher et al. (2012). They used the GEOS-Chem model with a slab-ocean module to simulate the impact of seasonal variability of Hg fluxes with river discharge. This simulation showed the importance of seasonality in external sources in causing seasonal variability not only in the surface ocean but also in the marine boundary layer Hg concentration due to the rapid interaction between the surface ocean and atmosphere. They thus highlighted the connectedness and fast response in the Arctic surface ocean. Zhang et al. (2015) and later Sonke et al. (2018), using a global biogeochemical model (MITgcm) but with a specific focus on the Arctic Ocean processes, also found that rivers are major drivers of seasonal variability in the surface ocean Hg concentrations. Measurements made since 2015 are consistent with these modeling results. For example, Charette et al. (2020) reported elevated Hg within the Transpolar Drift, a current that transports river-influenced Eurasian shelf waters and sea ice to the central Arctic Ocean.

Several modeling studies show that sea ice plays an important role in regulating the air-sea exchange of Hg. Fisher et al. (2012) first showed the importance of air-sea exchange as a mechanism that results in a rapid adjustment of the surface ocean Hg concentrations as the Hg influx to the surface ocean fluctuates (on seasonal scale). Zhang et al. (2015) reported that 80% of the riverine Hg input evades to the atmosphere once it reaches the Arctic Ocean. Air-sea exchange of Hg is greatly influenced by the fraction of open ocean. For example, Zhang et al. (2015) showed that the western Arctic Ocean has higher Hg concentrations than the eastern Arctic Ocean and proposed the difference is due to increased deposition because of more frequent AMDEs and greater summertime ice cover in the western Arctic Ocean. Two other modeling studies directly addressed the impact of declining ice cover and concluded that the loss will result in lower surface ocean Hg concentrations (Chen et al., 2015; Soerensen et al., 2016a). Soerensen et al. (2016a) showed that declining sea-ice area since the 1970s resulted in an increase in the net loss of Hg to the atmosphere due to the impact of evasion (reaching a relative difference in surface ocean concentrations of ~10% in 2010).

In addition to changes in sea-ice cover, other processes undergoing climate-driven shifts can influence the Arctic Hg cycle, such as air and seawater temperature or Arctic sea-ice regime shifts from multi-year to first-year ice dominance (Schartup et al., 2020). For example, Zhang et al. (2020) showed that heat transfers from rivers to estuaries increases Hg (0) evasion by accelerating snowmelt, and increasing transfer velocity of Hg(0) and turbulence. Fisher et al. (2013) used historic simulations from the GEOS-Chem global Hg model with a slab ocean module to analyze the drivers of interannual variability in Arctic atmospheric Hg. They found that climate related shifts such as high air temperatures, declining sea-ice area, warmer spring temperatures (Bekryaev et al., 2010) and increased cloudiness (Eastman and Warren, 2010) lead to lower fluxes of Hg from the atmosphere to the cryosphere and from the cryosphere to the ocean.

Until very recently, there were no high resolution MeHg concentrations profiles for the central Arctic Ocean (Heimbürger et al., 2015) and the drivers of Hg methylation are still virtually unknown. Because of these limitations, only three models include MeHg species in their simulations: the Soerensen et al. (2016a) box model and the two global biogeochemical models MITgcm and NEMO (Zhang et al., 2020; Semeniuk and Dastoor, 2017). Soerensen et al. (2016a) developed the first MeHg budget for the Arctic Ocean and concluded that most MeHg is produced in situ in subsurface ocean waters (20–200 m). Zhang et al. (2020) proposed that the MeHg concentrations in the top 100 m of ocean waters are higher in the Arctic (and Antarctic) than elsewhere because of lower demethylation rather than higher methylation. Semeniuk and Dastoor (2017) suggested that abiotic methylation driven by dissolved organic carbon could be important for MeHg production at depth. Because of the limited understanding of MeHg production in the Arctic Ocean, here we focus exclusively on changes in total Hg.

For this study, we conducted model simulations to quantify the impact of different policy scenarios (see Section 2) on the future total Hg concentrations in the Arctic Ocean with a focus on the change during the period 2015–2050. The goal was to compare the impact of management strategies for anthropogenic Hg emissions to the influence of climate change-driven changes in the Arctic ecosystem on seawater Hg concentrations. Based on the literature review of the existing model results (Table S2) and drivers identified in AMAP, 2021 (Chapter 5), we selected three quantifiable climate-related changes predicted to impact the Arctic Ocean Hg cycle in the coming decades: sea-ice cover, river discharge and net primary production (NPP). The simulations are performed with a low spatial resolution level (box model) to capture major impacts on the total Hg cycle in the Arctic Ocean.

4.1. Ocean model description

We perform the model simulations using a five-compartment box model (3 water column layers and shelf and deep ocean sediments; see Fig. 4). This is a simplified version of the Soerensen et al. (2016a) model that only computes inorganic Hg processes (Hg(II) and Hg(0)). A full description of the model parameterizations can be found in Soerensen et al. (2016a). Briefly, the model includes external Hg inputs such as atmospheric deposition, river discharge, erosion and snowmelt as well as ocean circulation. The internal processes considered are particle settling, diffusion, evasion and chemical transformation between Hg(II) and Hg(0). Process specific rates and/or fluxes are calculated using first order differential equations deduced from the present-day Hg budget presented in Soerensen et al. (2016a). For the climate change model runs, literature-derived climate variables are used to scale rates/fluxes to evaluate their projected impact on the Hg cycle. Atmospheric Hg deposition to the surface ocean is modeled as a direct flux to the surface water or deposition on sea ice. Thus, the relative change in the fraction of open ocean to sea ice influences Hg concentrations in the water and redox transformations. The extent of sea-ice coverage also impacts the release of Hg from the springtime/summertime meltwater and evasion of Hg(0).

The solids budget is based on Rachold et al. (2004) but modified to include changes in net primary production and in sea ice cover (Hill et al., 2013). The settling of suspended particles considers the fraction of solids remaining at each modeled depth in the water column after remineralization (Moran et al., 1997; Rachold et al., 2004; Cai et al., 2010). The fraction of solids from rivers and NPP remaining after remineralization at each depth is 50% in the surface ocean, 30% in the subsurface water and 1% in the deep ocean (Fig. 4). Solids from erosion are assumed not to remineralize. Hg settling is estimated based on the mass of settling particles and an average concentration of Hg in suspended solids found in the Arctic (Soerensen et al., 2016a). To estimate the impact of NPP on seawater concentrations, the model is run forced by past (1850–2015) relative changes and projected changes to 2050.

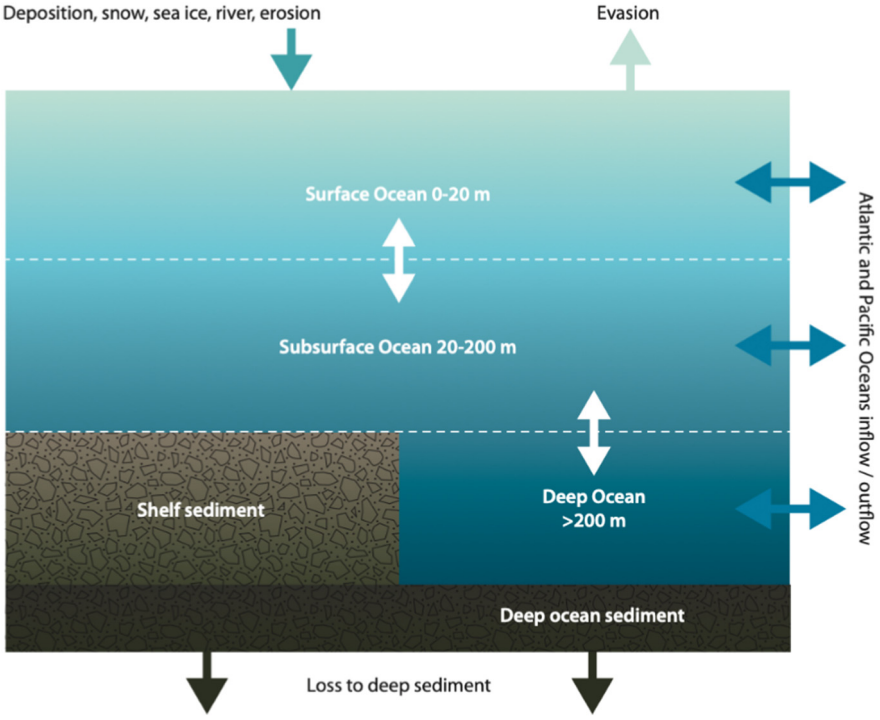

Fig. 4. Simplified layout of the five-compartments Arctic mercury box model. Detailed parameterization of external and internal processes can be found in Soerensen et al. (2016a).

The model is run from 1850 to 2015 to create a common starting point for the scenario simulations (Soerensen et al., 2016a). For each model run, the known variability in deposition, sea-ice area, NPP and river water discharge is included. The individual 2015–2050 climate scenarios are run while changing only one climate variable, while the others are kept constant at the 2015 level in order to be able to quantify the impact of each driver. A final run simulates the impact of all three climate variables simultaneously with constant deposition.

4.2. Future scenarios

Here we explore the relative influence of changing Hg deposition under policy scenarios described in Section 3 and of changing sea ice, riverine input, and NPP on Hg concentrations in the Arctic Ocean.

4.2.1. Sea ice scenario

This scenario examines the influence of changes in sea ice on the Hg ocean reservoir through simulating the relative change in the sea-ice covered area of the Arctic Ocean. The change between 1950 and the present day is based on observations (e.g., from the U.S. National Snow and Ice Data Center; NSIDC), while the future trend is based on the CMIP6 simulations under the SSP2-4.5 scenario where surface air temperatures increase by ~3 °C by 2100 (SIMIP, 2020). Fig. 5 shows that according to this projection the Arctic Ocean will have lost approximately 20% of its sea-ice cover by 2050 compared to 2015. Changes in sea-ice cover impact the exchange of Hg between seawater and the atmosphere as well as the amount of Hg that can be stored or released by the sea ice in the summer (Fisher et al., 2013; Zhang et al., 2015; Soerensen et al., 2016a; Agather et al., 2019; DiMento et al., 2019; Schartup et al., 2020). Sea ice also influences surface-water redox processes by controlling how much light penetrates the water column. We thus expect that the observed rapid decline in sea-ice volume and extent from the central Arctic Ocean will lead to lower seawater Hg concentrations. Reductions in sea-ice content track linear changes in global temperature and carbon dioxide emissions, although there is great uncertainty in the sensitivity of sea ice to warming (SIMIP, 2020).

4.2.2. Riverine input scenario

The riverine input scenario indicates the direction and proportional effect of an increase in external forcing from the terrestrial environment on ocean Hg concentrations, although it likely underestimates actual increases from terrestrial sources. Modeling studies described in AMAP (2021) (-Chapter 4) indicate that Arctic rivers contribute amounts of Hg to the Arctic Ocean that are of the same magnitude as atmospheric sources. Sonke et al. (2018) used a combination of field measurements and modeling to reduce the uncertainty on the current day riverine Hg flux into the Arctic Ocean, which they estimated to be 44 ± 4 Mg/y. However, this riverine flux of Hg is expected to increase because river water discharge has been

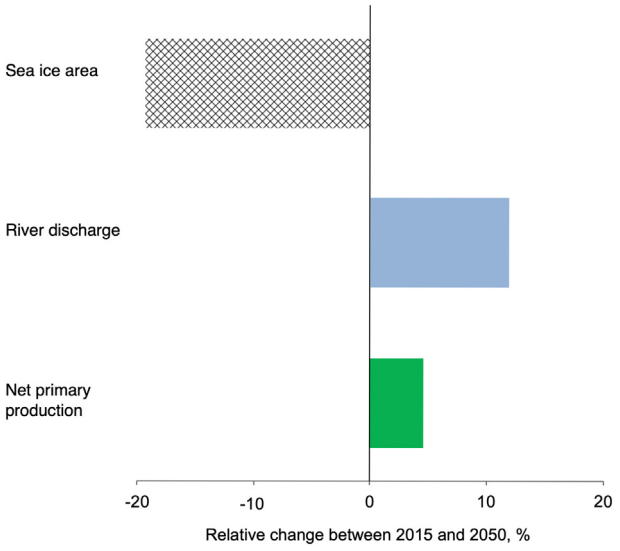

Fig. 5. Bars represent the relative change in sea-ice area (pattern), river discharge (blue) and net primary production (green) used in future scenario simulations between 2015 and 2050.

increasing since consistent monitoring began in 1930s (Peterson et al., 2002) and Hg laden permafrost thaw is expected to release increasingly larger amounts of Hg (Vonk et al., 2015; Schuster et al., 2018; Schaefer et al., 2020). To create the river scenario used in this section, we used discharge data covering the period from 1936 through to 1999 obtained from Peterson et al. (2002). Future trends were reported in Haine et al. (2015) for 1980 through to 2100 (2000–2010) reaching 5500 km^3/y by 2100. If Hg control policies are implemented, Hg deposition to the watershed should decline and decrease river Hg concentrations (with some time lag). On the other hand, thawing permafrost is likely to release stored Hg to rivers, thus increasing Hg concentrations in river discharge (Schuster et al., 2018; Koven et al., 2012; Schaefer et al., 2020). Because the overall result of these opposing forcings is unknown, we assume a constant Hg concentration in river water as discharge increases giving an overall increase in the Hg load from rivers. Fig. 5 shows an approximately 12% increase in the riverine discharge scenario between 2015 and 2050. This is within the range of the increased discharge observed between 1975 and 2015 (AMAP, 2021: Chapter 5).

4.2.3. Net Primary Production scenario

To address the impact of changing NPP on the ocean Hg reservoir, we use the most conservative projections of NPP increase in this scenario (about a 5% rise between 2015 and 2050; Fig. 5). Reduction in sea-ice coverage results in more light reaching the Arctic Ocean. This has been suggested to increase NPP, and most models agree that NPP will increase in the future. NPP has been shown to enhance algal scavenging of Hg in Arctic lakes and NPP is expected to increase the removal of Hg from the upper layers of the Arctic Ocean, thus reducing its bioavailability (Brazeau et al., 2013; Grasby et al., 2013; Soerensen et al., 2016b). However, no prior Arctic Ocean model simulations have investigated the importance of changes to the NPP. Expected future trends in NPP are less well constrained than sea-ice decline or river discharge (Vancoppenolle et al., 2013). Arrigo and van Dijken (2015) show a negative correlation between NPP and sea-ice cover (i.e., increasing NPP with decreasing sea-ice volume). However, NPP in the Arctic Ocean could also decrease if the nitrate supply is not large enough to sustain the excess growth. The CMIP5 performed simulations with 11 Earth system models between 1900 and 2100 and found conflicting results (Vancoppenolle et al., 2013). Overall, the models' mean increase in NPP is smaller (+58 TgC/y) than the increases predicted from simple linear extrapolations between NPP and sea-ice observations. For example, Arrigo and van Dijken (2011) calculated a 300 TgC/y increase in NPP between 1998 and 2009, and Arrigo and van Dijken (2015) reported a 30% increase between 1998 and 2012. Our model scenario does not account for the impact of higher NPP on the surface ocean chemistry.

4.3. Impact of anthropogenic mercury emission policies and delays in implementation on Arctic Ocean total mercury concentrations

We use the No Action, NP and MFR deposition scenarios to force the ocean model to predict changes in Hg concentrations for the surface, subsurface and deep Arctic Ocean in 2050 (Fig. 3). Fig. 6 presents the Arctic Ocean's response as the percentage change in concentrations in 2050 compared to 2015 due to the implementation of the various policy scenarios. In this simulation, all other parameters, including climate variables, are kept constant.

The No Action scenario results in a total Hg concentration increase ranging from 22% in the surface to almost 9% at depth by 2050. Under the most aggressive scenario, MFR-2020, concentrations decrease by 14%, 10% and 4% in the surface, subsurface and deep ocean, respectively, by 2050. Thus, the difference in response between the two extreme scenarios (No Action and MFR-2020) is 36% for the surface ocean and 13% for the deep ocean. These results are consistent with Chen et al. (2018) who found that the No Action scenario would result in a 9% increase in Hg mass, while a zero emissions scenario would lead to 10% reduction in Hg mass by 2050 for the entire Arctic Ocean (surface, subsurface and deep ocean reservoirs combined). The NP scenarios also result in total Hg declines in the surface and subsurface water layers, albeit more moderate, and in the deep ocean they result in very little change (from a 1% reduction to a 3% increase). The NP and MFR simulations show the importance of prompt action with the impact particularly visible in the surface ocean, which has a faster response time. In the surface ocean, where changes are overall smaller than in the atmosphere, Hg has a lifetime of about 10 years; thus, delaying implementation to 2035 results in 5% more Hg in the water by 2050 compared to policy implementation in 2020. The deep ocean, in which changes to concentration lag the surface ocean and where concentration has not reached a steady-state, mostly continues to see increases driven by legacy Hg inputs and only the MFR-2020 scenario offers a small trend reversal by 2050 (a 4% reduction).

4.4. Impact of climate variables on Arctic Ocean total mercury concentrations

Fig. 7 shows the impacts of changes in sea-ice cover, river discharge and NPP individually and combined on total Hg concentrations by 2050. In

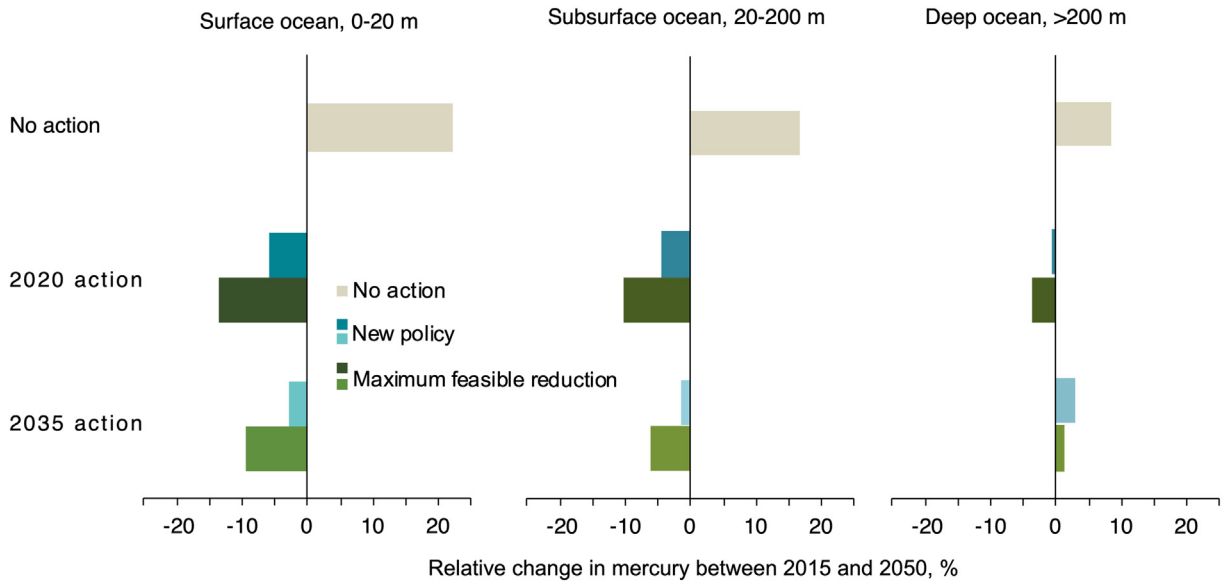

Fig. 6. Relative change in Arctic Ocean Hg concentrations between 2015 and 2050 in the surface (0–20 m, left panel), subsurface (20–200 m, middle panel) and deep ocean (<200 m, right panel), under the No Action (cream), New Policy (blue) and Maximum Feasible Reduction (green) scenarios implemented in 2020 and 2035.

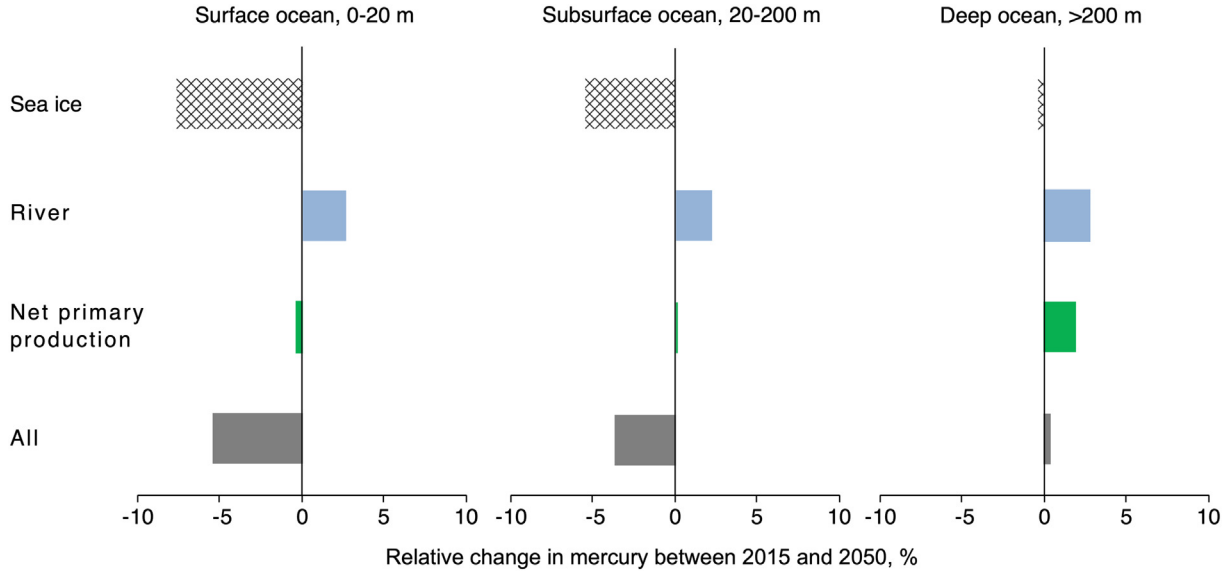

Fig. 7. Relative change in Arctic Ocean Hg concentrations between 2015 and 2050 in the surface (0–20 m, left panel), subsurface (20–200 m, middle panel) and deep ocean (<200 m, right panel), under four climate scenarios: sea ice (pattern), river discharge (blue), net primary production (green) and "all" which represents their combined impact (dark gray). For each model run, atmospheric depositions are kept constant at 2015 levels while the model is run forced by changes in one variable from 1850 to 2050. In the "all" scenario, sea ice, river discharge and net primary production change over time while deposition is kept constant at 2015 levels after 2015.

these simulations, the atmospheric deposition is kept constant at 2015 levels to be able to compare the influence of these drivers on Hg concentrations to the influence of policy scenarios and implementation delays shown in Fig. 6.

The role of sea-ice extent on the Hg cycle is multi-fold. It controls the amount of atmospheric Hg that deposits directly to the surface of the water column, sunlight penetration, air-sea exchange and Hg release from melting sea ice in the spring and summer. The model considers the combined influences of these processes and projects that the continued retreat of sea ice (an additional 20% by 2050) will reduce Hg concentrations in the Arctic Ocean. This is true for all depths, although the reduction is highest (−8%) in the surface ocean and smallest in the deep ocean (<1%) because of the lag time in the response. This decline in surface ocean Hg of 0.2% per year due to disappearing sea ice covered areas is in the same range as the decline calculated by Soerensen et al. (2016a) between 1975 and 2010, during which a loss of approximately 15% of sea-ice cover was observed.

The increased river discharge adds 2% to 3% to seawater Hg concentrations to all the water masses. This is because the model considers it to be a simple and uniform external input equivalent to atmospheric deposition. In reality, the impact of river discharge has a very different spatial distribution from atmospheric deposition, with a larger influence on shelves and near-shore areas. The river discharge increases by 12% by 2050 in this scenario (Fig. 5), which corresponds to ~3.3% of external inputs to the Arctic Ocean and is reflected in the change in seawater concentration.

Sea-ice retreat increases NPP (Arrigo and van Dijken, 2015) which in turn enhances particle settling and Hg scavenging (Soerensen et al., 2016b). The model estimates that the predicted 5% increase in NPP by 2050 (Fig. 5) will cause an increase in the removal of Hg from the surface ocean and slightly lower the concentration (<1%). Because the settling from the deep ocean to the seafloor is slow, some of this scavenged Hg accumulates in the deep ocean layer (Fig. 7). This causes the Hg concentration in the deep ocean to increase in this scenario by 2%. Overall, the predicted NPP effect is small, but this could be due to multiple assumptions made in this modeling. As the NPP projections are very uncertain, a conservative increase was used to drive the model (Vancoppenolle et al., 2013). For example, if NPP were to double by 2050 (Arrigo and van Dijken, 2011) the model calculates a much larger (7%) decrease in surface Arctic Ocean Hg concentration. In addition, the modeling described here relies on an older solids budget; a study by Tesán Onrubia et al. (2020) estimated a downward flux of particulate Hg using the radionuclide pair $^{234}Th/^{238}U$ coupled to particulate Hg/^{234}Th and found a larger sinking flux that could change the aforementioned estimates and the influence of increasing NPP.

We find that, of the 3 climate variables considered, the declining sea-ice cover exerts the strongest Hg reducing forcing on all layers of the Arctic Ocean, whereas river discharge exerts the largest increase, although smaller in absolute terms than sea ice. In the final combined scenario (with atmospheric deposition kept constant at 2015 levels), the surface and subsurface ocean layers see 5% and 4% Hg declines by 2050, respectively. The cumulative influence of these climate variables in the deep ocean is below a 1% increase. It should be noted that this model does not consider the impact of Hg that evades due to lower sea-ice cover on the atmospheric Hg levels and the potential local and global redeposition of this Hg (Chen et al., 2018). While we do not present an exhaustive list of climate drivers, the study shows their contrasting impacts on the Hg cycle in the Arctic Ocean. It also shows that our chosen climate drivers have a smaller influence on Hg concentrations in the Arctic Ocean than the influence of Hg anthropogenic emission control policies.

5. Conclusions and recommendations

We surveyed future projections of emissions and concentration changes in the Arctic atmosphere and ocean, and conducted a model-based assessment of projected changes in concentrations in the atmosphere and ocean in the short- and medium-term (to 2050). We assessed the implications of different emissions trajectories, and compared the relative importance of primary emissions changes, legacy emissions, and climate change to Arctic Hg concentrations.

The most aggressive global emissions reductions trajectories can reduce future Arctic Hg atmospheric concentrations both in the near- and medium-term. Different projections of future anthropogenic emissions globally exhibit a large range, including both substantial increases and decreases. Thus, different trajectories of global emissions changes can have correspondingly substantial effects on atmospheric concentrations in the Arctic. For deposition to the Arctic, the MFR scenario could lead to a 27% decrease relative to the present-day. Under the "No action" scenario, concentrations could increase, implying an even larger effect of emissions control policy. For ocean surface concentrations, this corresponds to a 36% difference in surface water Hg concentration between the two extreme estimates ("No action" and MFR-2020).

The changes in Hg deposition to the Arctic that are possible because of aggressive emissions reductions, however, may be substantially counteracted by the growing impact of continuing emissions if these changes are not implemented rapidly. Delaying emissions reduction measures until 2035 means that emissions in the intervening years could completely counteract the impacts of less ambitious emission cuts (the NP scenario), due to the continued cycling of these pre-2030 emissions globally. This underscores the large impacts of prompt action for changing Hg concentrations in the Arctic environment.

The magnitude of emissions-induced future changes in the Arctic atmosphere and ocean are likely to be substantial in comparison with climate-induced effects, especially for the ocean. For the atmosphere, the changes projected under different emissions scenarios relative to the present are comparable in magnitude over mid-latitudes to those calculated under future emissions scenarios, but no atmospheric model analyses have previously focused on the Arctic in particular.

Sensitivity scenarios for key climate parameters and their impact on ocean concentrations show that these effects are likely to be offsetting in different directions and overall have a smaller impact on Hg concentrations in the Arctic Ocean than the influence of anthropogenic Hg emission control policies. We modeled the impact of three climate variables individual and together – declining sea-ice cover, riverine discharge, and increased NPP. We show that sea ice cover exerts the strongest Hg reducing forcing on all layers of the Arctic Ocean, whereas river discharge exerts the largest increase. It is important to note that this model does not consider the impact of these climate variables on the biogeochemistry and speciation of Hg. Moreover, especially for assessing the impact of climate change in 2050 and beyond, we are also not considering that scenarios that project socio-economic activity associated with higher greenhouse gas emissions and thus a warmer climate would likely be associated with higher Hg emissions. For the atmosphere, as a result, it is likely that the higher-end estimates of Hg cycling changes under a warming climate would be associated also with larger direct emissions contributions. If climate change mitigation efforts continue, and proceed together with Hg mitigation, this implies that the relative impact of Hg emissions changes compared with climate impacts for the Arctic may be even larger than that simulated here.

Several areas of uncertainty affect our analysis of future changes across all timescales. For the short-term, the overall magnitude of emissions is uncertain, and different models vary in their estimates of regional source contributions to Arctic deposition (AMAP, 2021). In the medium-term, uncertain parameters in global biogeochemical cycle models, including global ocean processes, affect the magnitude of legacy emissions. For the longer-term, efforts to compare potential changes in Arctic Hg driven by climate and future Hg emissions in a more quantitative way should apply consistent projections of Hg emissions and future climate policy when assessing their relative magnitudes. Hg emissions projections that are fully consistent with the state-of-the-art scenarios used in climate modeling are currently not available, challenging researchers' abilities to assess and attribute potential changes in concentrations. Further development of emissions inventories and use of consistent climate projections in coupled atmosphere-ocean-land models will be necessary to better understand the importance of future emissions changes and to monitor the effectiveness of future controls.

Future research is necessary to better quantify the processes that influence the global transport, deposition, and cycling and transformations of Hg in the Arctic environment. Also, a better understanding and integration of the influence of climate sensitive variables, such as temperature, plankton size and distribution, or erosion, on Hg inputs and speciation are needed to improve ocean Hg modeling.

CRediT authorship contribution statement

NES and ATS conceptualized the research. ATS, ALS, HA performed the atmospheric and ocean modeling. ATS, ALS, HA and NES wrote the original draft. KB provided data for model evaluation. All authors edited, revised, and approved the manuscript.

Declaration of competing interest

The authors declare that they have no known competing financial interests or personal relationships that could have appeared to influence the work reported in this paper.

Acknowledgements

This work was supported by US National Science Foundation grants 2023046 to ATS and 1924148 to NES. HA received financial support from the Swiss National Science Foundation (grant no. 200021_188478) to finalize the manuscript.

Appendix A. Supplementary data

Supplementary data to this article can be found online at https://doi.org/10.1016/j.scitotenv.2022.155477.

References

Agather, A.M., Bowman, K.L., Lamborg, C.H., Hammerschmidt, C.R., 2019. Distribution of mercury species in the Western Arctic Ocean (U.S. GEOTRACES GN01). Mar. Chem. 216, 103686. https://doi.org/10.1016/j.marchem.2019.103686.

AMAP, 2021. Arctic Monitoring and Assessment Program 2021: Mercury in the Arctic.

AMAP/UN Environment, 2019. Technical Background Report for the Global Mercury Assessment 2018. Arctic Monitoring and Assessment Programme (AMAP), Oslo, Norway/UN Environment Programme (UNEP), Chemicals and Health Branch, Geneva Switzerland viii + 426pp.

Amos, H.M., Jacob, D.J., Streets, D.G., Sunderland, E.M., 2013. Legacy impacts of all-time anthropogenic emissions on the global mercury cycle. Glob. Biogeochem. Cycles 27, 410–421. https://doi.org/10.1002/gbc.20040.

Angot, H., Hoffman, N., Giang, A., Thackray, C.P., Hendricks, A.N., Urban, N.R., Selin, N.E., 2018. Global and local impacts of delayed mercury mitigation efforts. Environ. Sci. Technol. 52, 12968–12977. https://doi.org/10.1021/acs.est.8b04542.

Arrigo, K.R., van Dijken, G.L., 2015. Continued increases in Arctic Ocean primary production. Prog. Oceanogr. 136, 60–70.

Arrigo, K.R., van Dijken, G.L., 2011. Secular trends in Arctic Ocean net primary production. J. Geophys. Res. Oceans 116 (C9), C09011.

Bekryaev, R.V., Polyakov, I.V., Alexeev, V.A., 2010. Role of polar amplification in long-term surface air temperature variations and modern Arctic warming. J. Clim. 23, 3888–3906. https://doi.org/10.1175/2010JCLI3297.1.

Brazeau, M.L., Poulain, A.J., Paterson, A.M., Keller, W., Sanei, H., Blais, J.M., 2013. Recent changes in mercury deposition and primary productivity inferred from sediments of lakes from the Hudson Bay Lowlands, Ontario,Canada. Environ. Pollut. 173, 52–60. https://doi.org/10.1016/j.envpol.2012.09.017.

Cai, P., Rutgers van der Loeff, M., Stimac, I., Nöthig, E.-M., Lepore, K., Moran, S.B., 2010. Low export flux of particulate organic carbon in the central Arctic Ocean as revealed by 234Th:238U disequilibrium. J. Geophys. Res. Oceans 115 (C10), C10037.

Charette, M.A., Kipp, L.E., Jensen, L.T., Dabrowski, J.S., Whitmore, L.M., Fitzsimmons, J.N., et al., 2020. The transpolar drift as a source of riverine and shelf-derived trace elements to the central Arctic Ocean. J. Geophys. Res.-Oceans 125, e2019JC015920.

Chen, L., Wang, H.H., Liu, J.F., Tong, Y.D., Ou, L.B., Zhang, W., Hu, D., Chen, C., Wang, X.J., 2014. Intercontinental transport and deposition patterns of atmospheric mercury from anthropogenic emissions. Atmos. Chem. Phys. 14 (18), 10163–10176.

Chen, L., Zhang, W., Zhang, Y., Tong, Y., Liu, M., Wang, H., Xie, H., Wang, X., 2018. Historical and future trends in global source-receptor relationships of mercury. Sci. Total Environ. 610–611, 24–31.

Chen, L., Zhang, Y., Jacob, D.J., Soerensen, A.L., Fisher, J.A., Horowitz, H.M., Corbitt, E.S., Wang, X., 2015. A decline in Arctic Ocean mercury suggested by differences in decadal trends of atmospheric mercury between the Arctic and northern midlatitudes. Geophys. Res. Lett. 42, 6076–6083. https://doi.org/10.1002/2015GL064051.

Cole, A.S., Steffen, A., 2010. Trends in long-term gaseous mercury observations in the Arctic and effects of temperature and other atmospheric conditions. Atmos. Chem. Phys. 10 (10), 4661–4672.

Corbitt, E.S., Jacob, D.J., Holmes, C.D., Streets, D.G., Sunderland, E.M., 2011. Global source-receptor relationships for mercury deposition under present-day and 2050 emissions scenarios. Environ. Sci. Technol. 45 (24), 10477–10484.

Dastoor, A.P., Durnford, D.A., 2014. Arctic Ocean: is it a sink of source of atmospheric mercury? Environ. Sci. Technol. 48 (3), 1707–1717. https://doi.org/10.1021/es404473e.

Dastoor, A., Ryzhkov, A., Durnford, D., Lehnherr, I., Steffen, A., Morrison, H., 2015. Atmospheric mercury in the Canadian Arctic. Part II: insight from modeling. Sci. Total Environ. 509–510, 16–27. https://doi.org/10.1016/j.scitotenv.2014.10.112.

Dastoor, A., Angot, H., Bieser, J., et al., 2022a. Arctic mercury cycling. Nat. Rev. Earth Environ. https://doi.org/10.1038/s43017-022-00269-w.

Dastoor, A., Travnikov, Oleg, Angot, Hélène, Ryjkov, Andrei, Christensen, Jesper, John Chetelat, T.D., 2022b. What are the transport pathways, deposition to various surfaces, and deposition source attribution with respect to emissions? Sci. Total Environ. This issue.

DiMento, B.P., Mason, R.P., Brooks, S., Moore, C., 2019. The impact of sea ice on the air-sea exchange of mercury in the Arctic Ocean. Deep-Sea Res. I Oceanogr. Res. Pap. 144, 28–38. https://doi.org/10.1016/j.dsr.2018.12.001.

Douglas, T.A., Blum, J.D., 2019. Mercury isotopes reveal atmospheric gaseous mercury deposition directly to the Arctic coastal snowpack. Environ. Sci. Technol. Lett. 6, 235–242. https://doi.org/10.1021/acs.estlett.9b00131.

Eastman, R., Warren, S.G., 2010. Arctic cloud changes from surface and satellite observations. J. Clim. 23 (15), 4233–4242.

Fisher, J.A., Jacob, D.J., Soerensen, A.L., Amos, H.M., Steffen, A., Sunderland, E.M., 2012. Riverine source of Arctic Ocean mercury inferred from atmospheric observations. Nat. Geosci. 5. https://doi.org/10.1038/NGEO1478.

Fisher, J.A., Jacob, D.J., Soerensen, A.L., Amos, H.M., Corbitt, E.S., Streets, D.G., Wang, Q., Yantosca, R.M., Sunderland, E.M., 2013. Factors driving mercury variability in the Arctic atmosphere and ocean over the past 30 years. Glob. Biogeochem. Cycles 27. https://doi.org/10.1002/2013GB004689.

Giang, A., Stokes, L.C., Streets, D.G., Corbitt, E.S., Selin, N.E., 2015. Impacts of the Minamata Convention on mercury emissions and global deposition from coal-fired power generation in Asia. Environ. Sci. Technol. 49 (9), 5326–5335.

Grannas, A.M., Bogdal, C., Hageman, K.J., Halsall, C., Harner, T., Hung, H., Kallenborn, R., Klán, P., Klánová, J., Macdonald, R.W., Meyer, T., Wania, F., 2013. The role of the global cryosphere in the fate of organic contaminants. Atmos. Chem. Phys. 13, 3271–3305. https://doi.org/10.5194/acp-13-3271-2013.

Grasby, S.E., Sanei, H., Beauchamp, B., Chen, Z., 2013. Mercury deposition through the permo-triassic biotic crisis. Chem. Geol. 351, 209–216. https://doi.org/10.1016/j.chemgeo.2013.05.022.

Haine, T.W., Curry, B., Gerdes, R., Hansen, E., Karcher, M., Lee, C., Rudels, B., Spreen, G., de Steur, L., Stewart, K.D., Woodgate, R., 2015. Arctic freshwater export: status, mechanisms, and prospects. Glob. Planet. Chang. 125, 13–35.

Hayhoe, K., Edmonds, J., Kopp, R.E., LeGrande, A.N., Sanderson, B.M., Wehner, M.F., Wuebbles, D.J., 2017. Climate models, scenarios, and projections. In: Wuebbles, D.J., Fahey, D.W., Hibbard, K.A., Dokken, D.J., Stewart, B.C., Maycock, T.K. (Eds.), Climate Science Special Report: Fourth National Climate Assessment (NCA4). Volume I. U.S. Global Change Research Program, Washington, DC, USA, pp. 133–160.

Heimbürger, L.-E., Sonke, J.E., Cossa, D., Point, D., Lagane, C., Laffont, L., Galfond, B.T., Nicolaus, M., Rabe, B., van der Loeff, M.R., 2015. Shallow methylmercury production in the marginal sea ice zone of the central Arctic Ocean. Sci. Rep. 5, 10318.

Hill, V.J., Matrai, P.A., Olson, E., Suttles, S., Steele, M., Codispoti, L.A., Zimmerman, R.C., 2013. Synthesis of integrated primary production in the Arctic Ocean: II. In situ and remotely sensed estimates. Prog. Oceanogr. 110, 107–125.

IPCC, 2000. In: Nakicenovic, N., Swart, R. (Eds.), Special Report on Emissions Scenarios (SRES). A Special Report of Working Group III of the Intergovernmental Panel on Climate Change. Intergovernmental Panel on Climate Change (IPCC), Cambridge University Press, Cambridge, UK 570pp.

IPCC, 2014. In: Pachauri, R.K., Meyer, L.A. (Eds.), Climate Change 2014: Synthesis Report. Contribution of Working Groups I, II and III to the Fifth Assessment Report of the Intergovernmental Panel on Climate Change. Intergovernmental Panel on Climate Change (IPCC), Geneva, Switzerland 151pp.

Koven, et al., 2012. Analysis of permafrost thermal dynamics and response to climate change in the CMIP5 Earth System Models. Journal of Climate 26 (6), 1877–1900.

Kumar, A., Wu, S., Huang, Y., Liao, H., Kaplan, J.O., 2018. Mercury from wildfires: global emission inventories and sensitivity to 2000–2050 global change. Atmos. Environ. 173, 6–15.

Kumar, A., Wu, S., 2019. Mercury pollution in the Arctic from wildfires: source attribution for the 2000s. Environ. Sci. Technol. 53 (19), 11269–11275.

Lei, H., Wuebbles, D.J., Liang, X.-Z., Tao, Z., Olsen, S., Artz, R., Ren, X., Cohen, M., 2014. Projections of atmospheric mercury levels and their effect on air quality in the United States. Atmos. Chem. Phys. 14, 783–795.

Lim, A.G., Jiskra, M., Sonke, J.E., Loiko, S.V., Kosykh, N., Pokrovsky, O.S., 2020. A revised pan-Arctic permafrost soil Hg pool based on Western Siberian peat Hg and carbon observations. Biogeosciences 17, 3083–3097. https://doi.org/10.5194/bg-17-3083-2020.

Macdonald, et al., 2005. Climate change, risks and contaminants: A perspective from studying the Arctic. Hum. Ecol. Risk Assess. 11 (6), 1099–1104. https://doi.org/10.1080/10807030500346482.

Marelle, L., Raut, J.C., Law, K.S., Duclaux, O., 2018. Current and future Arctic aerosols and ozone from remote emissions and emerging local sources—modeled source contributions and radiative effects. J. Geophys. Res. Atmos. 123, 12942–12963. https://doi.org/10.1029/2018JD028863.

Moore, et al., 2014. Convective forcing of mercury and ozone in the Arctic boundary layer induced by leads in sea ice. Nature 506 (7486), 81–84.

Moran, S.B., Ellis, K.M., Smith, J.N., 1997. 234Th/238U disequilibrium in the central Arctic Ocean: implications for particulate organic carbon export. Deep-Sea Res. II Top. Stud. Oceanogr. 44 (8), 1593–1606.

Mulvaney, K.M., Selin, N.E., Giang, A., Muntean, M., Li, C.-T., Zhang, D., Angot, H., Thackray, C.P., Karplus, V.J., 2020. Mercury benefits of climate policy in China: addressing the Paris Agreement and the Minamata Convention simultaneously. Environ. Sci. Technol. 54 (3), 1326–1335.

Obrist, D., Kirk, J.L., Zhang, L., Sunderland, E.M., Jiskra, M., Selin, N.E., 2018. A review of global environmental mercury processes in response to human and natural perturbations: changes of emissions, climate, and land use. Ambio 47 (2), 116–140.

Olson, C., Jiskra, M., Biester, H., Chow, J., Obrist, D., 2018. Mercury in active-layer tundra soils of Alaska: concentrations, pools, origins, and spatial distribution. Glob. Biogeochem. Cycles 32, 1058–1073. https://doi.org/10.1029/2017GB005840.

Pacyna, E.G., Pacyna, J.M., Steenhuisen, F., Wilson, S., 2006. Global anthropogenic mercury emission inventory for 2000. Atmos. Environ. 40 (22), 4048–4063.

Pacyna, J.M., Travnikov, O., De Simone, F., Hedgecock, I.M., Sundseth, K., Pacyna, E.G., Steenhuisen, F., Pirrone, N., Munthe, J., Kindbom, K., 2016. Current and future levels of mercury atmospheric pollution on a global scale. Atmos. Chem. Phys. 16 (19), 12495–12511.

Peterson, B.J., Holmes, R.M., McClelland, J.W., Vörösmarty, C.J., Lammers, R.B., Shiklomanov, A.I., Shiklomanov, I.A., Rahmstorf, S., 2002. Increasing river discharge to the Arctic Ocean. Science 298, 2171–2173.

Rachold, V., Eicken, H., Gordeev, V.V., Grigoriev, M.N., Hubberten, H.-W., Lisitzin, A.P., Shevchenko, V.P., Schirrmeister, L., 2004. Modern terrigenous organic carbon input to the Arctic Ocean. Org. Carbon Cycle Arct. Ocean 33–55. https://doi.org/10.1007/978-3-642-18912-8_2.

Rafaj, P., Bertok, I., Cofala, J., Schöpp, W., 2013. Scenarios of global mercury emissions from anthropogenic sources. Atmos. Environ. 79, 472–479.

Rafaj, P., Cofala, J., Kuenen, J., Wyrwa, A., Zyśk, J., 2014. Benefits of European climate policies for mercury air pollution. Atmosphere 5 (1), 45–59.

Riahi, K., Van Vuuren, D.P., Kriegler, E., Edmonds, J., O'neill, B.C., Fujimori, S., Bauer, N., Calvin, K., Dellink, R., Fricko, O., Lutz, W., 2017. The Shared Socioeconomic Pathways and their energy, land use, and greenhouse gas emissions implications: an overview. Glob. Environ. Chang. 42, 153–168.

Schaefer, K., et al., 2020. Potential impacts of mercury released from thawing permafrost. Nat. Commun. 11 (1). https://doi.org/10.1038/s41467-020-18398-5.

Schartup, A.T., Soerensen, A.L., Heimbürger-Boavida, L.-E., 2020b. Influence of the Arctic sea-ice regime shift on sea-ice methylated mercury trends. Environ. Sci. Technol. Lett. 7, 708–713. https://doi.org/10.1021/acs.estlett.0c00465.

Schuster, P.F., Schaefer, K.M., Aiken, G.R., Antweiler, R.C., Dewild, J.F., Gryziec, J.D., Gusmeroli, A., Hugelius, G., Jafarov, E., Krabbenhoft, D.P., Liu, L., 2018. Permafrost stores a globally significant amount of mercury. Geophys. Res. Lett. 45 (3), 1463–1471.

Selin, N.E., 2018. A proposed global metric to aid mercury pollution policy. Science 360 (6389), 607–609.

Semeniuk, K., Dastoor, A., 2017. Development of a global ocean mercury model with a methylation cycle: outstanding issues. Glob. Biogeochem. Cycles 31, 400–433. https://doi.org/10.1002/2016GB005452.

SIMIP, 2020. Arctic Sea Ice in CMIP6. Geophys. Res. Lett. 47 (10). https://doi.org/10.1029/2019GL086749.

Soerensen, A.L., Jacob, D.J., Schartup, A.T., Fisher, J.A., Lehnherr, I., St. Louis, V.L., Heimbürger, L.-E., Sonke, J.E., Krabbenhoft, D.P., Sunderland, E.M., 2016. A mass budget for mercury and methylmercury in the Arctic Ocean. Glob. Biogeochem. Cycles 30. https://doi.org/10.1002/2015GB005280.

Soerensen, A.L., Schartup, A.T., Gustafsson, E., Gustafsson, B.G., Undeman, E., Björn, E., 2016b. Eutrophication increases phytoplankton methylmercury concentrations in a coastal sea—a baltic sea case study. Environ. Sci. Technol. 50, 11787–11796. https://doi.org/10.1021/acs.est.6b02717.

Sonke, J.E., Teisserenc, R., Heimbürger-Boavida, L.E., et al., 2018. Eurasian river spring flood observations support net Arctic Ocean mercury export to the atmosphere and Atlantic Ocean. Proc. Natl. Acad. Sci. U. S. A. 115, E11586–E11594. https://doi.org/10.1073/pnas.1811957115.

St Pierre, et al., 2018. Unprecedented Increases in Total and Methyl Mercury Concentrations Downstream of Retrogressive Thaw Slumps in the Western Canadian Arctic. Environ. Sci. Technol. 52 (24), 14099–14109. https://doi.org/10.1021/acs.est.8b05348.

Stern, Gary, et al., 2012. How does climate change influence arctic mercury? Sci. Total Environ., 22–42 https://doi.org/10.1016/j.scitotenv.2011.10.039.

Streets, D.G., Zhang, Q., Wu, Y., 2009. Projections of global mercury emissions in 2050. Environ. Sci. Technol. 43 (8), 2983–2988.

Tesán Onrubia, J.A., Petrova, M.V., Puigcorbé, V., et al., 2020. Mercury export flux in the Arctic Ocean estimated from 234Th/238U disequilibria. ACS Earth Space Chem. 4, 795–801. https://doi.org/10.1021/acsearthspacechem.0c00055.

Travnikov, O., Angot, H., Artaxo, P., Bencardino, M., Bieser, J., D'Amore, F., Dastoor, A., De Simone, F., DÍéguez, M.C., Dommergue, A., Ebinghaus, R., 2017. Multi-model study of mercury dispersion in the atmosphere: atmospheric processes and model evaluation. Atmos. Chem. Phys. 5271–5295.

Vancoppenolle, M., Bopp, L., Madec, G., Dunne, J., Ilyina, T., Halloran, P.R., Steiner, N., 2013. Future Arctic Ocean primary productivity from CMIP5 simulations: uncertain outcome, but consistent mechanisms. Glob. Biogeochem. Cycles 27 (3), 605–619.

Vonk, J.E., Tank, S.E., Bowden, W.B., Laurion, I., Vincent, W.F., Alekseychik, P., Amyot, M., Billet, M.F., Canario, J., Cory, R.M., Deshpande, B.N., 2015. Reviews and syntheses: effects of permafrost thaw on Arctic aquatic ecosystems. Biogeosciences 12 (23), 7129–7167.

Zhang, Y., Jacob, D.J., Dutkiewicz, S., Amos, H.M., Long, M.S., Sunderland, E.M., 2015. Biogeochemical drivers of the fate of riverine mercury discharged to the global and Arctic oceans. Glob. Biogeochem. Cycles 29. https://doi.org/10.1002/2015GB005124.

Zhang, Y., Soerensen, A.L., Schartup, A.T., Sunderland, E.M., 2020. A global model for methylmercury formation and uptake at the base of marine food webs. Glob. Biogeochem. Cycles 34. https://doi.org/10.1029/2019GB006348.